

Semantic-guided spatial relation and object co-occurrence modeling for indoor scene recognition

Chuanxin Song^a, Hanbo Wu^a, Xin Ma^{a,*}, Yibin Li^a

^a*Center for Robotics, School of Control Science and Engineering, Shandong University, Jinan, China*

Abstract

Exploring the semantic context in scene images is essential for indoor scene recognition. However, due to the diverse intra-class spatial layouts and the coexisting inter-class objects, modeling contextual relationships to adapt various image characteristics is a great challenge. Existing contextual modeling methods for indoor scene recognition exhibit two limitations: 1) During training, space-independent information, such as color, may hinder optimizing the network’s capacity to represent the spatial context. 2) These methods often overlook the differences in coexisting objects across different scenes, suppressing scene recognition performance. To address these limitations, we propose SpaCoNet, which simultaneously models the Spatial relation and Co-occurrence of objects based on semantic segmentation. Firstly, the semantic spatial relation module (SSRM) is designed to explore the spatial relation among objects within a scene. With the help of semantic segmentation, this module decouples the spatial information from the image, effectively avoiding the influence of irrelevant features. Secondly, both spatial context features from the SSRM and deep features from the Image Feature Extraction Module are used to distinguish the coexisting object across different scenes. Finally, utilizing the discriminative features mentioned above, we employ the self-attention mechanism to explore the long-range co-occurrence among objects, and further generate a semantic-guided feature representation for indoor scene recognition. Experimental results on three widely used scene datasets demonstrate the effectiveness and generality of the proposed method. The code will be made publicly

*Corresponding author

Email address: maxin@sdu.edu.cn (Xin Ma)

available after the blind review process is completed.

Keywords: Indoor scene recognition, Semantic spatial context, Object co-occurrence, Attention mechanism, Adaptive ambiguity processing

1. Introduction

Scene recognition is a fundamental research topic in computer vision, aimed at predicting the scene category of an image, such as "bedroom" and "beach." Although many studies have focused on outdoor scene recognition[1, 2], an increasing number of researchers have recently conducted research on indoor scene recognition[3, 4, 5, 6, 7] due to its wide range of applications in smart video intelligence, robotics and so on[8]. As shown in Fig. 1, compared with outdoor scene recognition, indoor scene recognition presents more significant challenges due to the intra-class diverse spatial layout and the coexisting objects in different scene categories. Therefore, it is crucial to develop effective methods for indoor scene representation.

Existing scene recognition methods can be broadly classified into handcrafted feature-based and deep learning-based methods. Hand-crafted features, such as LBP[9] and OTC[10], utilize color and texture to recognize scenes and have yielded noteworthy results. However, their limitation is that they only use low-level features such as shape and gradient information, which makes them unsuitable for dealing with large-scale datasets or complex scenes. Recently, Deep Neural Networks (DNNs) based methods attract a lot of interest and obtain higher performance, since DNNs can acquire a more advanced feature representation for images. However, the performance of DNNs for indoor scene recognition is still limited due to the complex relationships among objects within indoor scenes. Some recent studies[11, 12] that explore the scene essence also suggest that scene classification is closely related to the inter-object context it contains. Thus, fully exploiting the object information is crucial for recognizing indoor scenes. As shown in Fig. 1, the varying spatial layouts amplify the intra-class distinctions of indoor scenes, while the presence of coexisting objects in different indoor scenes easily leads to category confusion. Inspired by this phenomenon, we propose SpaCoNet, which aims to simultaneously model the **S**patial layout and long-range **C**o-occurrence

of objects for indoor scene recognition.



Fig. 1. Some examples of different scene datasets. Images in the bedroom and hospital room categories can easily be confused. Similar ambiguity can be found in the classroom and restaurant. In contrast, the simple composition makes the variation between the different outdoor scene categories quite obvious.

Several similar strategies have been proposed recently to obtain intra-scene object information to assist scene recognition, achieving encouraging results. To model the spatial context, [7] proposes to utilize the object-relation-object triplet to explore the spatial order relationships among objects. Approaches[13, 14] analyze the spatial metric relationships among object regions for scene recognition. However, it is noteworthy that spatial relationships encompass not only order and metric relationships but also topological relationships (e.g., the concept of a pillow being surrounded by a bed)[15], which are inherently more complex to formulate. Relying solely on artificial definitions is evidently insufficient for analyzing such diverse spatial relationships within scenes. Motivated by the powerful fitting ability of neural networks[16], this paper proposes using neural networks to adaptively model spatial relationships in an end-to-end manner. [13, 14] also assign semantic labels to the backbone features to analyze the spatial metric relationships among object features. However, the effectiveness of these methods mainly depends on the features extracted by the backbone network. It should be noted that space-irrelevant information, such as color, present in these features may impede the optimization of the network’s capacity to represent spatial context during training. In contrast, our objective is to thoroughly explore all

spatial relationships among objects in the scene. Accordingly, this paper proposes a Semantic Spatial Relation Module, which first decouples the spatial information from the image with the help of semantic segmentation, and then explores the spatial relationships among objects, thereby ensuring the purity of the network input, avoiding the negative effects of irrelevant information.

In addition to spatial relationships, object co-occurrence in different scenes is also a significant contributor to scene recognition. Some methods[17, 5, 7] conclude the discriminative objects associated with scene categories by computing the probability distribution of objects within scenes. However, the discriminative objects in some scenes may be the same (e.g., the bed in the bedroom and the bed in the hospital room shown in Fig. 1), which poses a significant challenge to the above methods. In this paper, we propose a novel idea to solve this problem inspired by an interesting phenomenon. Specifically, even if the discriminative objects in the bedroom and the hospital room are the same, humans can still easily identify the differences between these two scenes because the same objects exhibit different characteristics in different scene classes (e.g., apparent variances between the beds in the above two scenes). Building on this insight, before exploring co-occurrence among objects across scenes, we first assign relevant features of the input scene to objects, enabling the network to distinguish similar objects like humans do. However, since the same object has different characteristics in various scenes, manual statistical methods [17, 5] are no longer appropriate for exploring the co-occurrence. Fortunately, the advent of Transformer provides a flexible architecture with a multi-head attention mechanism, which can capture the long-range dependencies among sequential features. Several transformer-based methods[18, 19, 20, 21] consider the global interactions of local features with the attention mechanism to obtain discriminative features. Inspired by them, we introduce a global-local dependency encoder, which can establish long-range co-occurrence among object features in an end-to-end manner.

In summary, the main contributions of this paper are presented as follows.

1. We propose SpaCoNet, a framework that simultaneously models the **S**patial relation and **C**o-occurrence of objects for indoor scene recognition.

2. A semantic spatial relation module is designed to explore the spatial context among object regions, which decouples the spatial information from the image with the help of semantic segmentation, thus avoiding the negative effects of irrelevant features and ensuring high interpretability. In this module, we also design a simple yet efficient Adaptive Confidence Filter to alleviate the semantic ambiguity caused by limited segmentation precision.
3. We propose distinguishing the same objects in different scenes by assigning them scene-related features, as a basis for fully exploring the long-range co-occurrence among objects across scenes using attention mechanisms.
4. The effectiveness of the proposed approach is evaluated on three different scene datasets, namely MIT-67[3], SUN397[22], and Places365[23]. The experimental findings demonstrate the effectiveness and generality of our approach.

A preliminary version of this work was presented in the conference paper[24]. We make significant extensions from different aspects as follows: 1) We optimize the use of spatial relationships between semantic regions within scenes, and evaluate new datasets to demonstrate the generalization of the proposed approach; 2) We propose a richer type of semantic relationship, i.e., a long-range cooccurrence among objects, to provide more discriminative information; 3) We conduct comprehensive ablation studies for the global-local dependency encoder and different variants of the aggregation methods, to show the effectiveness of each new proposed module; 4) Visualizations for the learned SpaCoNet are provided to present the characteristics of the proposed method.

2. Related works

This section briefly reviews several related researches and examines the differences and connections between related works and our proposed approach.

2.1. Scene recognition

Conventional scene recognition methods usually rely heavily on handcrafted feature extraction. Gist of the scene proposes to use Generalized Search Trees (GIST) to generate a global low-dimensional representation for each image, but ignore the

local structure information of the scene[25]. To cope with this problem, some researchers focus on local visual descriptors (such as Local Binary Patterns(LBP)[9] and Oriented Texture Curves (OTC)[10]), and use the Bag-of-Visual-Word (BOVW)[26] to integrate these local visual descriptors into image representation, but do not take spatial structure information into account. For this reason, Spatial Pyramid Matching (SPM)[27] has been proposed as a component of BOVW, extracting subregions' features and compensating for the missing spatial structure information. Based on the above, Quattoni et al.[3] propose a prototype-based model for indoor scenes that combines local and global discriminative information. However, the features used by the above methods are hand-crafted and low-level, which is limited to distinguish blurred or high-similarity scenes.

In recent years, deep neural networks have made significant progress in computer vision. Several network architectures [28, 16] have been used to facilitate the development of image classification. Accordingly, many approaches[29, 23] attempt to extract visual representations for scene recognition through deep neural networks. For example, Dual CNN-DL[29] proposes a new dictionary learning layer to replace the traditional FCL and ReLu, which simultaneously enhances features' sparse representation and discriminative ability by determining the optimal dictionary. Lin et al.[30] propose to transform convolutional features to the ultimate image representation for scene recognition by a hierarchical coding algorithm. These methods utilize convolutional neural networks to extract scene representations, significantly improving the recognition results. However, they still fall far short of the results achieved in tasks such as image classification. This phenomenon might be due to the lack of effective distinction of co-existing objects within scenes by CNNs. With this in mind, several approaches employ the object information in the scene for scene recognition.

2.2. *Semantic segmentation-based modeling*

Semantic segmentation techniques, which can assign semantic labels to each pixel inside an image, have been widely used in diverse applications in recent years. Xu et al.[31] propose distinguishing the background and foreground through a semantic parsing network, and remedy the raised negative transfer caused by variant background to

address the challenge of person reidentification. SGUIE-Net[32] uses object information as high-level guidance to obtain visually superior underwater image enhancement by region-wise enhancement feature learning.

Since the classification of a scene is related to the objects it contains, several approaches[33, 14] have used the semantic segmentation result to provide auxiliary information for scene classification. In SAS-Net[33], the semantic features generated by the semantic segmentation score tensor are used to add weights to different positions of the feature map generated by the RGB image, so that the network pays more attention to the discriminative regions in the scene image. ARG-Net[14] detects the scene’s foreground and background regions through semantic segmentation technology, combining them with the feature map obtained by the backbone network to establish the context relationship between regional features. Besides exploring contextual relationships, there are some approaches[17, 4, 5] that propose to use the object co-occurrence across scenes for scene recognition. SDO[17] proposes to use the co-occurrence probability of objects in different scenes to find discriminative objects, so that the negative effects of co-occurring objects in multiple scenes can be excluded. Zhou et al.[5] use the probabilistic method to establish the co-occurrence relationship of objects across scenes, and combine the representative objects with the global representation of the scene to obtain a better scene representation.

However, due to the limited precision of semantic segmentation techniques, all semantic segmentation-based methods face the negative impact of semantic ambiguity. This issue is typically mitigated using confidence threshold[17, 14], but as the data volume increases, such methods become inflexible and have limited effectiveness. To address this issue, this paper proposes a simple yet effective method to adaptively filter ambiguous points based on each image’s specific state, achieving remarkable results.

2.3. *Attention mechanism-based modeling*

Since the attention mechanism and its variant, the Transformer, can effectively model long-range dependencies, it has been utilized in various applications. SCViT-Net[21] uses the multi-head self-attention mechanism to model the global interactions of the local structural features for remote sensing image classification. Wang

et al.[20] introduce a hybrid CNN-Transformer feature extraction network to combine local details, spatial context, and semantic information for visual place recognition. FCT-Net[19] proposes a Transformer-based framework that combines CNN to improve the discriminative ability of features for scene classification. Inspired by the methods above, in this paper, we explore the long-range co-occurrence of object semantic features within scenes using the multi-head self-attention mechanism.

3. Our method

In this section, we provide a detailed description for the proposed SpaCoNet, which consists of five modules. We will first outline the entire model and then introduce each module in five subsections.

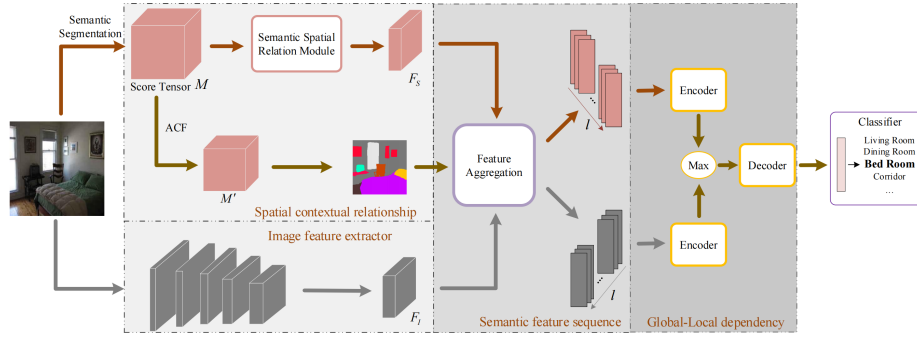


Fig. 2. Pipeline of the proposed SpaCoNet for indoor scene representation.

Fig. 2. shows the overall process of SpaCoNet. Our framework contains five modules: (a) semantic spatial relation module, (b) image feature extraction module, (c) semantic node feature aggregation module, (d) global-local dependency module, and (e) scene classifier. (a) provides feature maps that characterize the spatial relationships among object regions within the scene. (b) provides feature maps from PlacesCNN, which is pretrained on the large dataset Places365[23], to obtain the advanced representation of image information. The feature maps from (a) and (b), as well as the semantic segmentation label map of the input, are sent to (c). (c) performs feature aggregation on these two feature maps guided by the label map to generate two semantic feature sequences, which are sent to (d). (d) then explores the long-range co-occurrence among

semantic feature sequence through the attention mechanism and modifies the global features with the obtained information. Finally, the modified features are fed into (e) to predict the scene category.

3.1. Semantic Spatial Relation Module

Spatial relationships, as discussed in [15], encompass topological relationships (e.g., a pillow being surrounded by a bed), order relationships (e.g., a chair is behind a table), and metric relationships (e.g., the distance between an artboard and a person). Relying solely on artificial definitions is insufficient for analyzing such diverse spatial relationships within scenes. Motivated by the powerful fitting ability of neural networks[16], we propose the Semantic Spatial Relation module (SSRM) as an adaptive approach to model spatial relationships in an end-to-end manner.

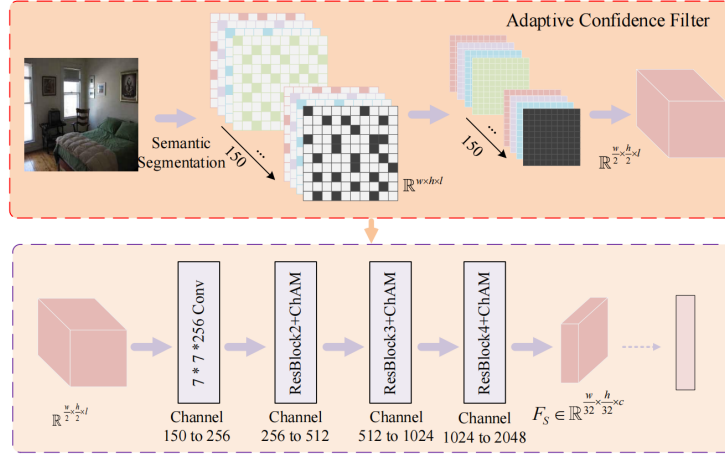


Fig. 3. Semantic Spatial Relation Module (SSRM), where the part surrounded by the red dashed box represents the confidence filtering stage, which is used to handle semantic ambiguities.

Firstly, to avoid the negative impact of space-irrelevant information during training, we input the given image $I \in \mathbb{R}^{w \times h \times 3}$ into a semantic segmentation network to obtain the semantic segmentation score tensor $M \in \mathbb{R}^{w \times h \times l} (l = 150)$ [34, 35]. The score tensor focuses solely on pure spatial information, filtering out non-essential elements. Then, we use M as the input for SSRM, ensuring that the module is devoid of spatially irrelevant information and can fully explore the spatial context. The SSRM generates

a spatial context feature $F_S \in \mathbb{R}^{\frac{w}{32} \times \frac{h}{32} \times c}$, which represents the concentrated representation of the spatial contextual information in I . Based on the ResNet50[16], we design a more suitable architecture for SSRM according to the specific characteristics of the segmentation score tensor. Compared with the original ResNet50, the proposed network is more efficient and requires less computing power. Fig. 3 illustrates the framework of the proposed SSRM.

Due to the precision limitation of the semantic segmentation network, errors in segmentation results are inevitable. Many existing methods[17, 14] have attempted to address this issue by implementing confidence thresholds to filter ambiguous points. Still, these methods are inflexible and have limited efficacy, especially when dealing with large datasets. In contrast, to alleviate the adverse effects caused by semantic ambiguity, we propose an Adaptive Confidence Filter (ACF) that is capable of dynamically adapting to the state of the image, which allows for flexible filtering of each semantic segmentation score tensor.

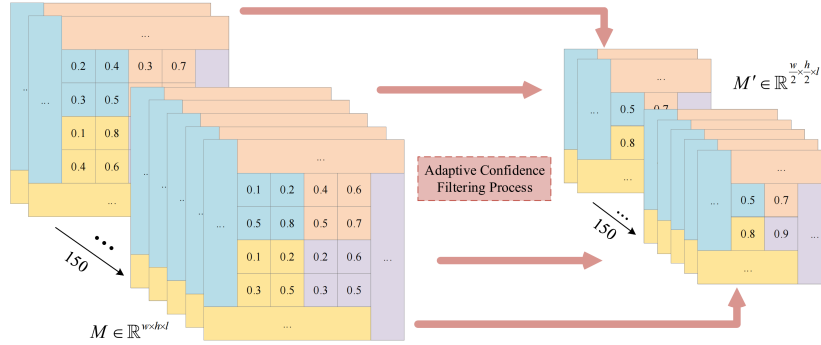


Fig. 4. An example of Adaptive Confidence Filter.

Specifically, ACF employs a filter with a kernel size of 2×2 to apply a smoothing process to each channel of M . For each domain the filter is applied to, ACF selects only the pixels with the highest confidence in its coverage, and generates the output $M' \in \mathbb{R}^{\frac{w}{2} \times \frac{h}{2} \times l}$ after processing all the channels of M . Fig. 4 illustrates an example of ACF. Compared to the segmentation map corresponding to M , in which internal points represent channels with the highest confidence within the $1 \times 1 \times l$ range, each pixel point in the segmentation map corresponding to M' represents the channel with the

highest confidence within the $2 \times 2 \times l$ range in which it is located. By leveraging the coverage of the discriminative domain instead of a fixed threshold, ACF filters the semantic segmentation map, enabling it to adjust to the unique characteristics of each image. Consequently, ACF improves the precision and generalizability of the semantic segmentation map. Moreover, ACF reduces the subsequent networks' input size, which reduces the computational cost of SSRM. We provide a comparative analysis of this concept in Section 4.3.1.

Next, the filtered semantic segmentation score tensor is processed using ResBlocks to explore spatial relation among object regions. ResBlocks includes *BasicBlocks* 2, 3, and 4 of the original ResNet50. Inspired by the fact that each channel value in $M'_{(i,j)}$ represents the predicted semantic probability of the corresponding pixel in image I [33, 34, 35], the Channel Attention Module (ChAM)[36] is introduced between ResBlocks to help the network to focus better on the critical semantic categories in the image.

Through exploring the spatial relation between object regions within M' , we can obtain the semantic-based spatial feature F_S , which encompasses comprehensive spatial context relationships.

3.2. Image Feature Extraction Module

In addition to spatial relationships, object co-occurrence across scenes is also a significant contributor to scene recognition. Of course, spatial relation also contains shallow multi-object co-occurrence information. Still, its focus is on exploring the positional relationships between objects, independent of the properties of the objects themselves, which is also why we use the decoupled M as the input to the SSRM to explore spatial relations. However, since M does not contain information about the characteristics of the objects themselves (color, texture, etc.), the SSRM lacks the ability to distinguish discriminative objects that may appear in different scenes, leading to under-exploration of object co-occurrence. Therefore, we propose an Image Feature Extraction Module (IFEM) for I to extract the complete image deep feature F_I . In this way, we can use F_I and F_S to link scene-related features with objects in subsequent modules, which allows us to fully explore the co-occurrence among objects within scenes.

Specifically, to fully use the information contained in an image, we propose to combine the SSRM with PlacesCNN, which serves as the Image Feature Extraction Module. The PlacesCNN used in this study consists of an almost complete ResNet50 architecture pretrained on the Places365 dataset[23]. Notably, we excluded the pooling layer from the architecture since it causes translation invariance, leading to the blurring of distinctions between various node features in the top-level semantic feature layer[37]. This blurring hinders the exploration of the global-local dependencies that follow. Therefore, we remove it to enhance the model’s performance in identifying and distinguishing such dependencies.

Given an image $I \in \mathbb{R}^{w \times h \times 3}$, IFEM generates an advanced deep feature $F_I \in \mathbb{R}^{\frac{w}{16} \times \frac{h}{16} \times c}$. The feature F_S and F_I are then forwarded into the semantic node feature aggregation module to link scene-related features with objects. Note that for tractability, we interpolate F_S to the same resolutions as F_I using the Bilinear interpolation algorithm.

3.3. Semantic node feature aggregation module

To differentiate the same objects across various scenes, we propose the semantic node feature aggregation module, which allocates objects with input scene-related features. By successively feeding spatial features F_S and deep features F_I to this module, we can obtain their respective semantic feature sequences.

For each image, we first obtain its semantic segmentation score tensor M from the SSRM, and generate the label map L from the probabilistic relationships within M . L enables us to extract the object information corresponding to each point in F_S and F_I . However, two issues arose:

1. Semantic ambiguity issue: Due to the limited precision of semantic segmentation, there can be errors in L , which may negatively affect subsequent works.
2. Resolution mismatch issue: The resolution of L is the same as the resolution of the input image, which is different from the resolution of the feature map.

To address these issues, we perform feature aggregation using the method described below, and the framework of this module is illustrated in Fig. 5.

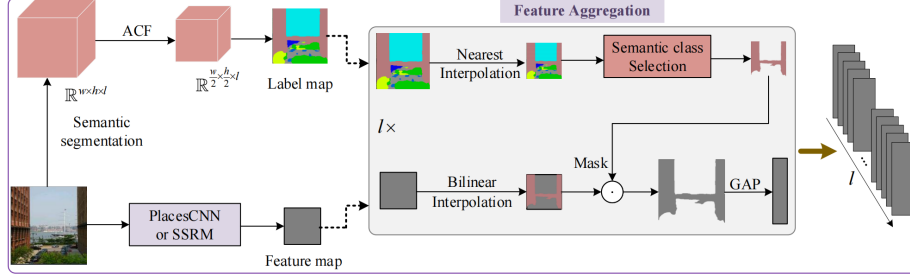


Fig. 5. The aggregation process of the Semantic Node Feature Aggregation Module for image features or spatial features. Note that this module handles these two feature maps separately.

For the Semantic ambiguity issue, we first apply the proposed ACF on the score tensor M to obtain M' . Subsequently, the refined tensor is used to generate the label map $L' \in \mathbb{R}^{\frac{w}{2} \times \frac{h}{2} \times l}$. In this way, we enhance the confidence level of the segmentation results.

For the Resolution mismatch issue, after obtaining L' , we use the nearest-neighbor interpolation algorithm to reduce its resolution to be consistent with the feature map F_I and F_S .

Subsequently, for each object o in l semantic categories, we generate a binary map L^o , as follows:

$$L_{i,j}^o = \begin{cases} 1, & L'_{i,j} = o \\ 0, & L'_{i,j} \neq o \end{cases} \quad (1)$$

We apply the binary map L^o over the feature map F_I and F_S , respectively, to extract the image features and spatial features related to object o . Then, we perform average pooling to obtain the deep feature vector $x_{rgb}^i \in \mathbb{R}^c$ and the spatial feature vector $x_{spa}^i \in \mathbb{R}^c$ of object o , which can be expressed as:

$$\begin{aligned} x_{rgb}^i &= \text{AveragePooling}(F_I \odot L^o) \\ x_{spa}^i &= \text{AveragePooling}(F_S \odot L^o) \end{aligned} \quad (2)$$

where \odot represents the Hadamard product.

Finally, the feature vectors stack together to form the deep aggregation feature $X_{rgb} \in \mathbb{R}^{l \times c}$ and the spatial aggregation feature $X_{spa} \in \mathbb{R}^{l \times c}$. The above process can

be formulated as follows:

$$\begin{aligned} X_{rgb} &= \text{concat}(x_{rgb}^0, x_{rgb}^1, x_{rgb}^2, \dots, x_{rgb}^{149}) \\ X_{spa} &= \text{concat}(x_{spa}^0, x_{spa}^1, x_{spa}^2, \dots, x_{spa}^{149}) \end{aligned} \quad (3)$$

Both X_{rgb} and X_{spa} are then fed into the Global-Local Dependency Module to explore the co-occurrence among semantic feature sequences.

3.4. Global-Local Dependency Modeling

Since the same object has different characteristics in various scenes, manual methods are no longer appropriate for exploring the co-occurrence among semantic feature sequences. To address this issue, we propose this module to establish a long-range correlation among semantic feature sequences by utilizing the attention mechanism. This relationship can then be used to modify the global feature representation.

To be specific, from the semantic node feature aggregation module, we get the deep feature sequence $X_{rgb} \in \mathbb{R}^{l \times c}$ and the spatial feature sequence $X_{spa} \in \mathbb{R}^{l \times c}$. Since our goal is to use the long-range cooccurrence among semantic feature sequences to modify the global representation, we make changes to the two feature sequences by using their respective global features as feature nodes, which is obtained by performing global average pooling on F_I and F_S , and thus obtain $X_{rgb}^1 \in \mathbb{R}^{(l+1) \times c}$ and $X_{spa}^1 \in \mathbb{R}^{(l+1) \times c}$.

$$\begin{aligned} X_{rgb}^1 &= \text{concat}(X_{rgb}, \text{GlobalAvgPooling}(F_I)) \\ X_{spa}^1 &= \text{concat}(X_{spa}, \text{GlobalAvgPooling}(F_S)) \end{aligned} \quad (4)$$

Meanwhile, considering the necessity of recording object semantic categories corresponding to each node feature, position embedding $P_{emb}^{rgb} \in \mathbb{R}^{(l+1) \times c}$ and $P_{emb}^{spa} \in \mathbb{R}^{(l+1) \times c}$ are further added to generate coded semantic feature sequences $X_{spa}^2 \in \mathbb{R}^{(l+1) \times c}$ and RGB feature sequence $X_{rgb}^2 \in \mathbb{R}^{(l+1) \times c}$. Hence, the inputs of two Encoders are formulated as follows:

$$\begin{aligned} X_{rgb}^2 &= X_{rgb}^1 + P_{emb}^{rgb} \\ X_{spa}^2 &= X_{spa}^1 + P_{emb}^{spa} \end{aligned} \quad (5)$$

Considering the disparities between these two feature sequences, we first explore their internal correlations individually, and then combine them to explore the intrinsic relationship of the overall information. The overall process is shown in Fig. 6.

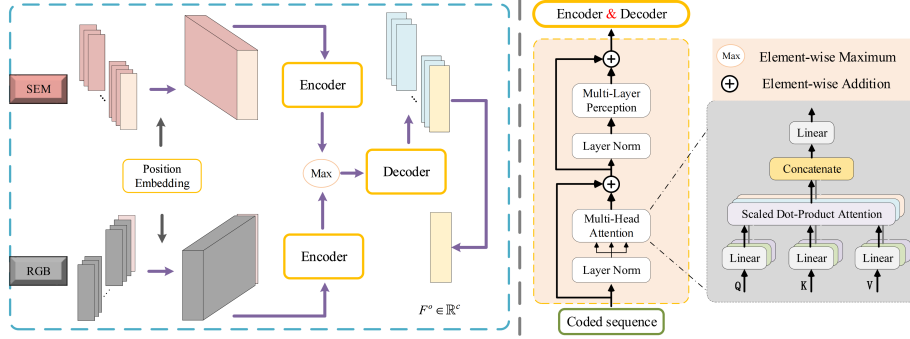


Fig. 6. Detailed structure of Global-Local Dependency Module.

We employ the attention mechanism to explore the long-range dependencies among local semantic feature nodes and between them and the global feature node. Inspired by Vision Transformer[18], an Encoder block consists of three main components: Layer normalization, Multi-head Self-Attention (MSA), and Multi-Layer Perceptron (MLP). Layer normalization is used to normalize and smooth data distribution, thereby improving the model’s generalization ability. The MSA follows it. Next, a residual connection is employed to convey information to alleviate overfitting. Afterward, Layer normalization is applied again, and the output of the Encoder block is obtained through MLP. The entire operation of the Encoder for processing the image aggregation feature $X_{rgb}^2 \in \mathbb{R}^{(l+1) \times c}$ and the spatial aggregation feature $X_{spa}^2 \in \mathbb{R}^{(l+1) \times c}$ is represented by follows:

$$\begin{aligned}
 X_{rgb}^3 &= X_{rgb}^2 + MSA(LN(X_{rgb}^2)) \\
 X_{rgb}^4 &= X_{rgb}^3 + MLP(LN(X_{rgb}^3)) \\
 X_{spa}^3 &= X_{spa}^2 + MSA(LN(X_{spa}^2)) \\
 X_{spa}^4 &= X_{spa}^3 + MLP(LN(X_{spa}^3))
 \end{aligned} \tag{6}$$

With the Encoder, we individually explore the long-range dependencies among the internal nodes of X_{rgb}^2 and X_{spa}^2 . Subsequently, we merge them by taking the element-wise Maximum:

$$X_o = \text{Max}(X_{spa}^4, X_{rgb}^4) \tag{7}$$

To better utilize the long-range dependency among nodes for scene representation, the output X_o is input to the Decoder to mitigate the disparities between image features

and spatial features and explore the overall information’s intrinsic relationships. The structure of the Decoder is similar to that of the Encoder and can be formulated as follows:

$$\begin{aligned} X_o^1 &= X_o + MSA(LN(X_o)) \\ X_o^2 &= X_o^1 + MLP(LN(X_o^1)) \end{aligned} \quad (8)$$

With the implementation of the Encoder and Decoder, we establish a robust long-range co-occurrence among all feature nodes. This integration process generates an optimized representation X_o^2 .

3.5. Scene Recognition Module

To optimize the scene representation, we employ attention mechanisms (Encoder and Decoder) to model the long-range dependency between global node and local nodes. To prevent over-fitting, we only adopt a one-layer Encoder and one-layer Decoder. After the Global-Local Dependency Modeling, we obtain the optimized representation X_o^2 . In classification processing, we extract the fully modified global feature node $F_o \in \mathbb{R}^c$ from X_o^2 as the final global representation (as shown in Fig. 6). These representations are fed into a fully connected network to obtain the final scene prediction, and the cross entropy function is used as the final loss:

$$L = - \sum_{n=1}^N y_i \log \frac{\exp(F_o(n))}{\sum_{m=1}^N \exp(F_o(m))} \quad (9)$$

where y is the ground truth and F_o is the output of this module.

4. Experiment

This section begins by presenting the benchmark datasets and performing ablation experiments to assess the impact of each module on the proposed method. Subsequently, we compare the proposed method with the state-of-the-art methods.

4.1. Datasets

MIT-67 dataset[3] consists of 67 indoor scene classes with a total of 15620 images, and each scene category contains at least 100 images. Following the recommendations by the authors[3], each class has 80 images for training and 20 images for testing. The

evaluation of the MIT dataset is challenging due to the large intra-class variation of indoor scenes.

SUN397[22] is a large dataset covering indoor and outdoor scenes. It contains 397 scene categories spanning 175 indoor scene categories and 220 outdoor scene categories, where each category contains at least 100 RGB images. In this study, we focus on the 175 indoor scene categories to evaluate our proposed approach. Following the evaluation protocol of the original paper[22], we randomly select 50 images from each scene class for training and another 50 for testing.

Places365 Dataset[23] is one of the largest scene recognition datasets, which includes about 1.8 million training images and 365 scene categories. This paper uses a simplified version, and only indoor scene categories are considered. To ensure a fair comparison with other indoor scene recognition methods[5], we used the same two scene class settings as them, namely Places365-7 and Places365-14. Places 365-7 contains seven indoor scenes: Bath, Bedroom, Corridor, Dining Room, Kitchen, Living Room, and Office. Places 365-14 contain 14 indoor scenes: Balcony, Bedroom, Dining Room, Home Office, Kitchen, Living Room, Staircase, Bathroom, Closet, Garage, Home Theater, Laundromat, Playroom, and Wet Bar. For the test set, we use the same setup as the official dataset[23].

4.2. Implementation details

Vision Transformer Adapter[34] that is pretrained on ADE20K dataset[35] is used as the semantic segmentation network. Given an image $I \in \mathbb{R}^{w \times h \times 3}$, its output is a score tensor $M \in \mathbb{R}^{w \times h \times l}$. This tensor can be used to generate the semantic label map $L \in \mathbb{R}^{w \times h}$ for I . The semantic prediction probability of location (i, j) in I is denoted by $M_{i,j} \in \mathbb{R}^{1 \times 1 \times l}$, where l represents the number of semantic labels ($l = 150$). In L , each pixel (i, j) is assigned a value L_{ij} , representing the semantic label of its corresponding pixel in the input image.

In order to thoroughly explore the spatial information in the input scene, it is essential to eliminate the impact of spatially irrelevant information on the network parameters when training the SSRM. As a result, a two-stage training procedure is implemented. Initially, we train the SSRM and IFEM separately. Subsequently, in the

second stage, we fix the weights of SSRM and IFEM and train the succeeding modules only. To ease the training process, we use ALI-G[38] to optimize the network parameters. ALI-G requires only an initial learning rate hyperparameter, which is set to 0.1 in all our experiments. In the second stage of training, to prevent over-fitting, the dropout regularization function is used in the final classifier with an omission probability of 0.8.

Thanks to PyTorch and SAS-Net [33], our method is implemented under their open-source framework. When evaluating the final performance, the standard 10-crop testing method[33, 39] is used for comparison with other methods.

4.3. Ablation analysis

In this part, we conduct ablation studies to evaluate the effectiveness of the proposed method.

4.3.1. Evaluation of the Semantic Spatial Relation Module

In this subsection, we evaluate the proposed SSRM on the MIT-67 and SUN397 datasets, and study the effect of the Adaptive Confidence Filter (ACF) on the recognition performance. The experimental results are presented in Table 1.

Table 1: Ablation results for different architectures for the SSRM

Architecture	Pretraining	MIT-67	SUN397	Flops(G)
resnet50	Scratch	64.403	50.529	27.2
4*4ACF + resnet50	Scratch	70.149	52.894	9.31
2*2ACF + resnet50	Scratch	69.627	53.035	9.31
resnet50_ChAM	Scratch	69.851	54.624	27.3
4*4ACF + resnet50_ChAM	Scratch	73.284	57.4	9.32
2*2ACF + resnet50_ChAM	Scratch	74.403	58.329	9.32
#2*2ACF + resnet50_ChAM	Places365	81.642	66.953	9.32

indicates that the model’s parameters are pretrained on Places365.

As shown in Table 1, filtering the semantic segmentation score tensor by ACF significantly improves recognition performance. When compared to inputting the original score tensor, the use of ACF in SSRM increases the recognition accuracy by 3.43% to 5.75% on MIT-67 and 2.365% to 3.705% on SUN397, while reducing the number of Flops by 17.89G. Additionally, ChAM further improves the accuracy of SSRM

with only a slight increase in Flops. Next, we investigate the impact of using ACF with different filtering domains on the recognition performance of SSRM. Our results show that using a $2*2$ ACF improves the accuracy of SSRM on MIT-67 and SUN397 by 1.12% and 0.929%, respectively, compared to using a $4*4$ ACF. This phenomenon suggests that while ACF reduces the negative impact of semantic ambiguity, it may also cause the input tensor to lose some object information. Therefore, when selecting the filter domain size of ACF, both the loss of object information and the presence of semantic ambiguity should be considered. However, it is worth noting that even though $4*4$ ACF results in more object information being lost, it still leads to a notable improvement of 3.43% and 2.776% in the accuracy of SSRM on MIT-67 and SUN397 datasets, respectively, which also indicates the importance of ACF in SSRM. Furthermore, we pretrain the SSRM on the Places365 dataset, achieving higher accuracy as demonstrated in the last row of Table 1.

4.3.2. Evaluation of different methods of feature aggregation

Combining the label map generated by the semantic segmentation and the feature map output by the backbone is essential for the semantic node aggregation module. The output (i.e., the semantic feature sequence) of this module directly influences the exploration of feature dependencies by the subsequent module, so the preliminary experiments are used to select the appropriate aggregation mode. To generate a suitable semantic feature sequence, we try a series of methods to integrate the label map and feature map, as shown in Table 2. Among them, *filtering* represents using ACF with the specified kernel size to filter the semantic segmentation score tensor, in the same way as the disambiguation filtering process in SSRM. *Nearest* means that the label map is interpolated to the specified size using nearest-neighbor interpolation, *Bilinear* means that the feature map is interpolated to the specified size using bilinear interpolation. For the sake of clarity in our presentation, we have assigned numbers to each of the aggregation methods. In this part, we first combine the output of SSRM and IFEM directly through Maximum and feed it to the classifier, using the result as the baseline, numbered as experiment 0.

As shown in Table 2, our approach consistently outperforms the baseline regardless

Table 2: Ablation results for different feature aggregation methods

Experiment	Score map	Label map	Feature map	MIT-67
0	-	-	-	88.731
1	-	<i>Nearest</i> to 14 * 14	-	89.851
2	2 * 2 <i>filtering</i>	<i>Nearest</i> to 14 * 14	-	90.746
3	4 * 4 <i>filtering</i>	<i>Nearest</i> to 14 * 14	-	90.149
4	-	-	<i>Bilinear</i> to 224 * 224	89.776
5	2 * 2 <i>filtering</i>	-	<i>Bilinear</i> to 112 * 112	90.224
6	4 * 4 <i>filtering</i>	-	<i>Bilinear</i> to 56 * 56	90.299
7	-	<i>Nearest</i> to 56 * 56	<i>Bilinear</i> to 56 * 56	90.075
8	2 * 2 <i>filtering</i>	<i>Nearest</i> to 56 * 56	<i>Bilinear</i> to 56 * 56	90.672

of the method used to aggregate the label map and feature map. This phenomenon suggests that Global-Local Dependency Modeling can obtain more discriminative scene representations. Moreover, upon experiments 1, 2, and 3; experiments 4, 5, and 6; and experiments 7 and 8, we observe that using the ACF on the score tensor consistently yields better results than using the original score tensor, aligning with the phenomenon observed in Table 1, further highlighting the superiority of the ACF in methods that utilize semantic segmentation. Additionally, comparing experiments 2 and 5 with experiments 3 and 6, it can be seen that using a 4 * 4 filter domain produces slightly weaker results than using a 2 * 2 filter domain, echoing the results presented in Table 1, again indicating the need to consider both disambiguation filtering and preservation of object information in the image when processing the score tensor using ACF.

Upon comparing experiments 2, 5, and 8, it is evident that finer semantic label assignment to features (i.e., interpolation of the feature map to a larger size) hurts final scene recognition. This phenomenon may be due to the interpolation algorithm causing a shift in feature position, which increases the possibility of assigning wrong semantic labels to features. Additionally, the comparison between experiments 5 and 6 also confirms this conclusion, where the large interpolation range results in a 2*2ACF filtered score tensor producing lower recognition than a 4*4ACF filtered score tensor, a result that should have been the opposite. Fortunately, using un-interpolated feature maps expedites the processing of this module. In summary, we finally choose the configu-

ration from experiment 2 to generate the feature sequence. Specifically, the 2*2ACF is first used to process the score tensor to generate a suitable label map. This label map is interpolated to the size of the feature map by nearest-neighbor interpolation. Finally, the label map and feature map are combined to produce the final semantic feature sequences.

4.3.3. Evaluation of different Encoder combination methods

Table 3: Ablation results for different Encoder combination methods

Method	MIT-67	SUN397
Product	89.925	75.965
Concatenation	90.299	75.859
Addition	90.373	75.965
Maximum	90.746	76.153

To explore the complementary information of the features generated by IFEM and SSRM, we compare four different Encoder combination methods, namely, Product, Concatenation, Addition, and element-wise Maximum. Table 3 illustrates the results on the MIT-67 and SUN397 datasets. The element-wise maximum combination method outperforms the alternative methods. Compared to the concatenation methods, the maximum method consumes fewer computational resources while achieving higher performance. Compared to the product and addition methods, the maximum method consumes the same computational resources while preserving the key information more cleanly, which allows the Decoder to decode dependencies in greater depth. In summary, we finally choose the element-level Maximum to combine the encoded features.

4.3.4. Network components analysis

We present a detailed ablation study of our method on the MIT-67 dataset in Table 4. We evaluate the effect of four components: PlacesCNN (baseline), Semantic spatial relation module, Encoder, and Decoder (Global-Local dependency module). In this part, we average the output features of PlacesCNN and use them as inputs to the classifier to obtain the classification results as the baseline. The results in Table 4 demonstrate that all the proposed modules positively boost the final recognition result.

Table 4: Ablation study of all components

PlacesCNN	SSRM	Encoder	Decoder	Accuracy
✓	-	-	-	84.970
-	✓	-	-	81.642
✓	✓	-	-	88.731
✓	✓	✓	-	90.075
✓	✓	✓	✓	90.746
Improvement Over Baseline (PlacesCNN)				5.776

In Table 4, the best results are marked in bold and show improvements of up to 5.776% over the baseline. Moreover, it could be observed that compared to the baseline, the accuracy is improved by 3.761% after incorporating the spatial contextual information extracted by SSRM into the network, and if the Encoder and Decoder fuse the long-range dependencies among objects on top of this, the accuracy can be improved again by 2.015%. Also, for the Encoder-Decoder, we try using only the output of the Encoder without the Decoder for scene recognition, yielding slightly lower results than those produced using the full Encoder-Decoder. This phenomenon is because the Decoder mitigates the differences in modal features between PlacesCNN and SSRM, thus better exploring the complementary information between them.

4.3.5. Feature visualization

Table 5: Ablation study of feature visualization

Method	MIT-67	Places365_7	Places365_14	SUN397
Baseline (PlacesCNN)	84.970	93.0	87.643	73.129
Ours	90.746	94.286	89.714	76.153

To better understand the learned feature representation, we evaluate our model and the baseline (PlacesCNN) on the test sets of MIT-67, Places365_7, Places365_14, and SUN397. The results of these evaluations are presented in Table 5. Additionally, we extract the features that will be fed into the classifier and use t-SNE to visualize them by plotting their 2-dimensional representations in Fig. 7. Each point represents an image, and points with the same color indicate images of the same category. The

first row of Fig. 7 shows the visualization of the output features from PlacesCNN, while the second row shows the visualization of the features output by our method. As demonstrated in Table 5 and Fig. 7, the proposed method significantly reduces the differences among scenes of the same category and increases the differences among scenes of different categories. By leveraging the spatial contextual relationships and long-range dependency among objects within scenes, our method is able to learn a more effective feature representation and achieve better performance.

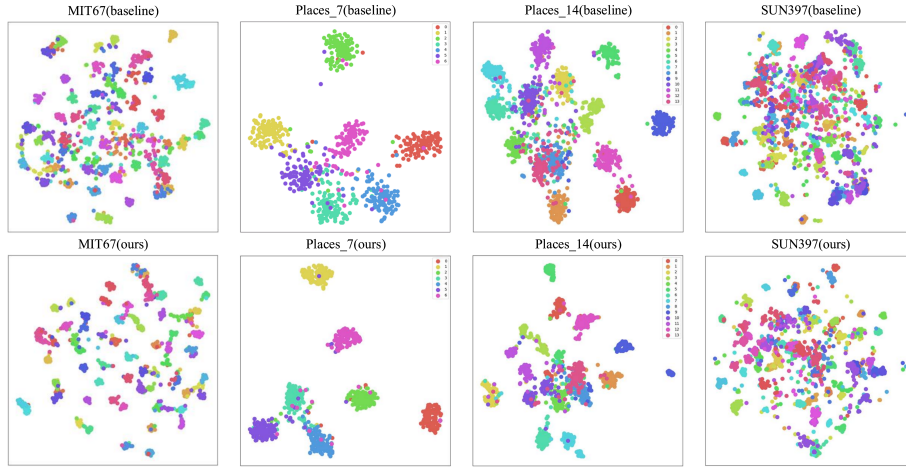


Fig. 7. Feature distributions of scene categories (different colors representing different categories).

4.4. Comparison with state-of-the-art methods

To demonstrate the superior performance of our method, we compare SpaCoNet with existing state-of-the-art methods on MIT-67, Places-7, Places-14, and SUN397 datasets. The results are presented in Tables 6, 7 and 8. It is observed that our SpaCoNet outperforms most existing methods. Compared to the methods[17, 4, 33, 14, 40, 5] that utilize object information for scene recognition, our method gains better performance, demonstrating that it is effective to exploit the spatial contextual relationships and long-range dependency among objects. Furthermore, our method outperforms current multi-branch-based approaches[33, 5, 41, 42, 43], which aim to obtain multi-scale information of the scene. This phenomenon highlights the effectiveness of using object information as an additional source. Moreover, while some methods aim

to improve accuracy by increasing the input size[39, 13, 14, 41, 42, 43], our proposed method achieves superior performance using a 224×224 input size, resulting in lower consumption of arithmetic power. Thus, our experiments confirm the superiority and generalization of the proposed method for indoor scene recognition.

Table 6: State-of-the-art results on MIT-67 dataset

Approaches	Publication	Network Input Size	Accuracy
Places365+VGGNet16[23]	TPAMI'18	224×224	76.53
Dual CNN-DL[29]	AAAI'18	224×224	76.56
NNSD+ICLC[30]	TMM'20	224×224	84.3
Multi-Resolution CNNs[39]	TIP'17	336×336	86.7
SDO[17]	PR'18	224×224	86.76
SAS-Net[33]	PR'20	224×224	87.1
CCF-Net[43]	KBS'21	512×512	87.3
DeepScene-Net[44]	Expert Syst. Appl'22	224×224	71.0
ARG-Net[14]	TMM'22	448×448	88.13
PL + AP + AI + IM[42]	TMM'19	448×448	88.06
LGN[13]	TIP'20	448×448	88.06
MR-Net[41]	Appl. Soft Comput'22	448×448	88.08
FCT-Net[19]	IJMIR'22	224×224	89.17
CSDML[45]	PR'22	224×224	88.28
CSRRM[24]	IJCNN'23	224×224	88.731
Ours	-	224×224	90.746

Table 7: State-of-the-art results on Places365-14 and Places365-7 dataset.

Approaches	Publication	Network Input Size	Places-14	Places-7
Word2Vec[6]	ICRA'18	224×224	83.7	-
Deduce[4]	IROS'19	224×224	-	88.1
BORM-Net[5]	IROS'21	224×224	85.8	90.1
OTS-Net[40]	IROS'21	224×224	85.9	90.1
CSRRM[24]	IJCNN'23	224×224	88.714	93.429
Ours	-	224×224	89.714	94.286

Table 8: State-of-the-art results on SUN397 dataset.

Approaches	Publication	Network Input Size	Accuracy
Places365+VGGNet16[23]	TPAMI'18	224×224	63.24
Dual CNN-DL[29]	AAAI'18	224×224	70.13
NNSD+ICLC[30]	TMM'20	224×224	64.78
Multi-Resolution CNNs[39]	TIP'17	336×336	72.0
SDO[17]	PR'18	224×224	73.41
SAS-Net[33]	PR'20	224×224	74.04
ARG-Net[14]	TMM'22	448×448	75.02
PL + AP + AI + IM[42]	TMM'19	448×448	74.12
LGN[13]	TIP'20	448×448	73.85
MR-Net[41]	Appl. Soft Comput'22	448×448	73.98
FCT-Net[19]	IJMIR'22	224×224	76.06
AdaNFF[2]	PR'22	256×256	74.18
Ours	-	224×224	76.153

5. Conclusions

In this paper, we propose a framework, SpaCoNet, to simultaneously model the **S**patial relation and **C**o-occurrence of objects for indoor scene recognition. Initially, we introduce a semantic spatial region module to model the spatial contextual relationships within a scene, in which an adaptive confidence filter is introduced to mitigate the negative impact of errors in the semantic segmentation results. Additionally, to explore co-occurrence among objects across scenes and distinguish the same objects in different scenes, we reformulate these objects as feature nodes, use attention mechanisms to model the long-range co-occurrence among object semantic features, and generate discriminative scene representation. Our approach is shown to be more competitive than existing approaches through comprehensive experiments.

However, the performance of the proposed method exhibits limitations due to the semantic segmentation technique used. Specifically, the segmentation technique used in this study is capable of segmenting 150 semantic objects; however, it does not cover all objects present in the scene, which is one of the reasons why we incorporate global features into the semantic feature sequence. Two potential strategies can be considered to address this issue. The first strategy is to train segmentation techniques that can effectively segment a larger number of semantic objects. However, this strategy requires

significant effort to annotate the dataset, making it a resource-intensive endeavor. Alternatively, the second strategy is to use an unsupervised or semi-supervised approach to enable the network to autonomously recognize objects within the scene, which is a direction we plan to explore in the future.

Acknowledgment

This work was jointly supported by the Key Development Program for Basic Research of Shandong Province under Grant ZR2019ZD07, the National Natural Science Foundation of China-Regional Innovation Development Joint Fund Project under Grant U21A20486, the Fundamental Research Funds for the Central Universities under Grant 2022JC011.

References

- [1] X. Zhu, J. Men, L. Yang, K. Li, Imbalanced driving scene recognition with class focal loss and data augmentation, *International Journal of Machine Learning and Cybernetics* 13 (10) (2022) 2957–2975.
- [2] Z. Zou, W. Liu, W. Xing, Adanff: A new method for adaptive nonnegative multi-feature fusion to scene classification, *Pattern Recognition* 123 (2022) 108402.
- [3] A. Quattoni, A. Torralba, Recognizing indoor scenes, in: 2009 IEEE conference on computer vision and pattern recognition, IEEE, 2009, pp. 413–420.
- [4] A. Pal, C. Nieto-Granda, H. I. Christensen, Deduce: Diverse scene detection methods in unseen challenging environments, in: 2019 IEEE/RSJ International Conference on Intelligent Robots and Systems (IROS), IEEE, 2019, pp. 4198–4204.
- [5] L. Zhou, J. Cen, X. Wang, Z. Sun, T. L. Lam, Y. Xu, Borm: Bayesian object relation model for indoor scene recognition, in: 2021 IEEE/RSJ International Conference on Intelligent Robots and Systems (IROS), IEEE, 2021, pp. 39–46.

- [6] B. X. Chen, R. Sahdev, D. Wu, X. Zhao, M. Papagelis, J. K. Tsotsos, Scene classification in indoor environments for robots using context based word embeddings, in: 2018 International Conference on Robotics and Automation (ICRA) Workshop, 2018.
- [7] X. Song, S. Jiang, B. Wang, C. Chen, G. Chen, Image representations with spatial object-to-object relations for rgb-d scene recognition, *IEEE Transactions on Image Processing* 29 (2019) 525–537.
- [8] L. Xie, F. Lee, L. Liu, K. Kotani, Q. Chen, Scene recognition: A comprehensive survey, *Pattern Recognition* 102 (2020) 107205.
- [9] T. Ojala, M. Pietikainen, T. Maenpaa, Multiresolution gray-scale and rotation invariant texture classification with local binary patterns, *IEEE Transactions on pattern analysis and machine intelligence* 24 (7) (2002) 971–987.
- [10] R. Margolin, L. Zelnik-Manor, A. Tal, Otc: A novel local descriptor for scene classification, in: *Computer Vision–ECCV 2014: 13th European Conference, Zurich, Switzerland, September 6–12, 2014, Proceedings, Part VII* 13, Springer, 2014, pp. 377–391.
- [11] M. A. Islam, M. Kowal, S. Jia, K. G. Derpanis, N. D. Bruce, Global pooling, more than meets the eye: Position information is encoded channel-wise in cnns, in: *Proceedings of the IEEE/CVF International Conference on Computer Vision*, 2021, pp. 793–801.
- [12] J. Qiu, Y. Yang, X. Wang, D. Tao, Scene essence, in: *Proceedings of the IEEE/CVF conference on computer vision and pattern recognition*, 2021, pp. 8322–8333.
- [13] G. Chen, X. Song, H. Zeng, S. Jiang, Scene recognition with prototype-agnostic scene layout, *IEEE Transactions on Image Processing* 29 (2020) 5877–5888.
- [14] H. Zeng, X. Song, G. Chen, S. Jiang, Amorphous region context modeling for scene recognition, *IEEE Transactions on Multimedia* 24 (2020) 141–151.

- [15] M. Egenhofer, A mathematical framework for the definition of topological relations, in: Proc. the fourth international symposium on spatial data handing, 1990, pp. 803–813.
- [16] K. He, X. Zhang, S. Ren, J. Sun, Deep residual learning for image recognition, in: Proceedings of the IEEE conference on computer vision and pattern recognition, 2016, pp. 770–778.
- [17] X. Cheng, J. Lu, J. Feng, B. Yuan, J. Zhou, Scene recognition with objectness, *Pattern Recognition* 74 (2018) 474–487.
- [18] A. Dosovitskiy, L. Beyer, A. Kolesnikov, D. Weissenborn, X. Zhai, T. Unterthiner, M. Dehghani, M. Minderer, G. Heigold, S. Gelly, J. Uszkoreit, N. Houlsby, An image is worth 16x16 words: Transformers for image recognition at scale, *ICLR* (2021).
- [19] Y. Xie, J. Yan, L. Kang, Y. Guo, J. Zhang, X. Luan, Fct: fusing cnn and transformer for scene classification, *International Journal of Multimedia Information Retrieval* (2022) 1–8.
- [20] Y. Wang, Y. Qiu, P. Cheng, J. Zhang, Hybrid cnn-transformer features for visual place recognition, *IEEE Transactions on Circuits and Systems for Video Technology* (2022).
- [21] P. Lv, W. Wu, Y. Zhong, F. Du, L. Zhang, Scvit: A spatial-channel feature preserving vision transformer for remote sensing image scene classification, *IEEE Transactions on Geoscience and Remote Sensing* 60 (2022) 1–12.
- [22] J. Xiao, J. Hays, K. A. Ehinger, A. Oliva, A. Torralba, Sun database: Large-scale scene recognition from abbey to zoo, in: 2010 IEEE computer society conference on computer vision and pattern recognition, IEEE, 2010, pp. 3485–3492.
- [23] B. Zhou, A. Lapedriza, A. Khosla, A. Oliva, A. Torralba, Places: A 10 million image database for scene recognition, *IEEE transactions on pattern analysis and machine intelligence* 40 (6) (2017) 1452–1464.

- [24] C. Song, X. Ma, Srrm: Semantic region relation model for indoor scene recognition, in: 2023 International Joint Conference on Neural Networks (IJCNN), 2023, pp. 01–08. doi:10.1109/IJCNN54540.2023.10191605.
- [25] A. Oliva, Gist of the scene, in: Neurobiology of attention, Elsevier, 2005, pp. 251–256.
- [26] L. Fei-Fei, P. Perona, A bayesian hierarchical model for learning natural scene categories, in: 2005 IEEE Computer Society Conference on Computer Vision and Pattern Recognition (CVPR’05), Vol. 2, IEEE, 2005, pp. 524–531.
- [27] S. Lazebnik, C. Schmid, J. Ponce, Beyond bags of features: Spatial pyramid matching for recognizing natural scene categories, in: 2006 IEEE computer society conference on computer vision and pattern recognition (CVPR’06), Vol. 2, IEEE, 2006, pp. 2169–2178.
- [28] A. Krizhevsky, I. Sutskever, G. E. Hinton, Imagenet classification with deep convolutional neural networks, Communications of the ACM 60 (6) (2017) 84–90.
- [29] Y. Liu, Q. Chen, W. Chen, I. Wassell, Dictionary learning inspired deep network for scene recognition, in: Proceedings of the AAAI conference on artificial intelligence, Vol. 32, 2018.
- [30] L. Xie, F. Lee, L. Liu, Z. Yin, Q. Chen, Hierarchical coding of convolutional features for scene recognition, IEEE Transactions on Multimedia 22 (5) (2019) 1182–1192.
- [31] S. Xu, L. Luo, J. Hu, B. Yang, S. Hu, Semantic driven attention network with attribute learning for unsupervised person re-identification, Knowledge-Based Systems 252 (2022) 109354.
- [32] Q. Qi, K. Li, H. Zheng, X. Gao, G. Hou, K. Sun, Sguie-net: Semantic attention guided underwater image enhancement with multi-scale perception, IEEE Transactions on Image Processing 31 (2022) 6816–6830.

- [33] A. López-Cifuentes, M. Escudero-Vinolo, J. Bescós, Á. García-Martín, Semantic-aware scene recognition, *Pattern Recognition* 102 (2020) 107256.
- [34] Z. Chen, Y. Duan, W. Wang, J. He, T. Lu, J. Dai, Y. Qiao, Vision transformer adapter for dense predictions, in: *ICLR*, 2023.
- [35] B. Zhou, H. Zhao, X. Puig, S. Fidler, A. Barriuso, A. Torralba, Scene parsing through ade20k dataset, in: *Proceedings of the IEEE conference on computer vision and pattern recognition*, 2017, pp. 633–641.
- [36] S. Woo, J. Park, J.-Y. Lee, I. S. Kweon, Cbam: Convolutional block attention module, in: *Proceedings of the European conference on computer vision (ECCV)*, 2018, pp. 3–19.
- [37] J. T. Springenberg, A. Dosovitskiy, T. Brox, M. Riedmiller, Striving for simplicity: The all convolutional net, *ICLR Workshop* (2015).
- [38] L. Berrada, A. Zisserman, M. P. Kumar, Training neural networks for and by interpolation, in: *International conference on machine learning*, PMLR, 2020, pp. 799–809.
- [39] L. Wang, S. Guo, W. Huang, Y. Xiong, Y. Qiao, Knowledge guided disambiguation for large-scale scene classification with multi-resolution cnns, *IEEE Transactions on Image Processing* 26 (4) (2017) 2055–2068.
- [40] B. Miao, L. Zhou, A. S. Mian, T. L. Lam, Y. Xu, Object-to-scene: Learning to transfer object knowledge to indoor scene recognition, in: *2021 IEEE/RSJ International Conference on Intelligent Robots and Systems (IROS)*, IEEE, 2021, pp. 2069–2075.
- [41] C. Lin, F. Lee, L. Xie, J. Cai, H. Chen, L. Liu, Q. Chen, Scene recognition using multiple representation network, *Applied Soft Computing* 118 (2022) 108530.
- [42] H. Zeng, X. Song, G. Chen, S. Jiang, Learning scene attribute for scene recognition, *IEEE Transactions on Multimedia* 22 (6) (2019) 1519–1530.

- [43] C. Sitaula, S. Aryal, Y. Xiang, A. Basnet, X. Lu, Content and context features for scene image representation, *Knowledge-Based Systems* 232 (2021) 107470. doi:<https://doi.org/10.1016/j.knosys.2021.107470>.
- [44] P. S. Yee, K. M. Lim, C. P. Lee, Deepscene: Scene classification via convolutional neural network with spatial pyramid pooling, *Expert Systems with Applications* 193 (2022) 116382.
- [45] Y. Wang, P. Liu, Y. Lang, Q. Zhou, X. Shan, Learnable dynamic margin in deep metric learning, *Pattern Recognition* 132 (2022) 108961.